Accuracy and Speed Considerations of a New Numerical Method for Modeling Cardiac Excitation

D Allexandre, NF Otani

Department of Biomedical Engineering, Case Western Reserve University, Cleveland, OH, USA

Abstract

A fast algorithm called the modified backward Euler (mBE) method, an explicit, variable timestep method, has been developed. Despite its explicit nature, the algorithm is unconditionally stable, allowing the use of timesteps several orders of magnitude larger than the timestep limit imposed by forward Euler methods. A guard cell algorithm also allows the use of timesteps larger than those imposed by the Courant Friedrich Levy (CFL) stability condition. The algorithm was applied to a two-dimensional tissue using the advanced Luo-Rudy ventricular cell model. Characteristic properties of action potential (AP) propagation including velocity, AP amplitude and duration, maximum membrane voltage and $\dot{V}_{max}$ were computed versus computational speed and compared to those obtained from a forward Euler fixed timestep (FEFT) method. Overall, for a given accuracy in velocity of 1% to 3%, the computational speed was increased by a factor of 30 to 40 over the FEFT, while the other errors were kept below 1%.

1. Introduction

Several methods have been developed in recent years to simulate and study the propagation properties of multi-dimensional cardiac tissue [1, 2, 3, 4]. The drive towards the development of more efficient methods is constantly fuelled by the desire to simulate larger tissue size using more and more detailed ionic cell models such as the Luo-Rudy model (LRd) [5]. Such an endeavor is, however, challenged and limited by the presence of severe numerical stability constraints, the large temporal and spatial dynamic variability of excitable tissue, and the extensive calculation associated with ionic currents. The large disparity in time constants is often addressed through the use of variable timestep explicit methods. Unfortunately, the efficiency of conventional explicit methods such as the forward Euler (FE) method is seriously limited by a timestep cap, which must be imposed in order to keep the diffusion calculation stable. This problem is often handled by the use of implicit or semi-implicit methods such as the Crank-Nicholson or alternate-direction implicit (ADI) methods. However one limitation of all implicit methods is the time synchronicity of all the cells required for matrix inversion. This dictates that a single timestep be used for the whole system at any given time, which in turn is limited by the smallest timestep required at any point in the system. Such condition affect significantly the efficiency. Various methods have attempted to take advantage of the stability property of implicit methods along with the flexibility of explicit methods by using independent timesteps for the diffusion and ionic currents and/or by calculating them at alternating times [4, 3, 2]. Nevertheless, the constraints of conventional explicit and implicit methods are still present, although to a lesser extent.

We propose to overcome such limitations by developing a highly stable explicit method called the modified backward Euler (mBE) method. Its explicit nature allows the use of a continuous, locally varying timestep algorithm based only on local accuracy criteria. A simple and flexible "guard cell" algorithm has also been developed to control the spatial timestep gradient. This algorithm allows timesteps larger than those imposed by the CFL stability condition. It also creates a zone with small timesteps at the foot of the action potential (AP) to improve the propagation velocity accuracy. We first present the method and the guard cell algorithm. We then apply the method to a tissue composed of ventricular cells using the LRd cell model, and compare the method's computational speed to that of the FEFT.

2. The mBE method

In one dimension, the membrane potential equation takes the form,

$$\partial_t V = D\partial_x^2 V + f(V, X) \tag{1}$$

where f is a function representing the local dynamics of each cell and X stands for all the other dynamical variables besides V. Our method was obtained by modifying the backward Euler method, which, when applied to Equation 1, takes the form,

$$\begin{aligned} V_k^{n+1} &= V_k^n + D\Delta t_k^n \frac{\tilde{V}_{k-1}^{n+1} - 2V_k^{n+1} + \tilde{V}_{k+1}^{n+1}}{\Delta x^2} \\ &\quad + \Delta t f(V_k^n, x_k^n) \end{aligned} \tag{2}$$

where the subscript k refers to the spatial grid point located at x_k, the superscript n refers to the time index, Δt_k^n to the timestep $t_k^{n+1} - t_k^n$, and $\tilde{V}_{k'}^{n+1}$ to the linear extrapolation (or interpolation) of V at time t_k^{n+1} of the central node. Specifically, $\tilde{V}_{k+1}^{n+1}$ is expressed as:

$$\tilde{V}_{k+1}^{n+1} = V_{k+1}^p + (V_{k+1}^p - V_{k+1}^{p-1}) \frac{(t_k^{n+1} - t_{k+1}^p)}{\Delta t_{k+1}^{p-1}} \qquad (3)$$

A similar expression applies to node $k-1$. Note that, since the membrane voltage at each node is calculated asynchronously, different time indices m and p need to be used for the latest values of the $(k-1)$st and $(k+1)$st adjacent nodes respectively. At every iteration, the algorithm looks for the earliest grid point in time and advances it by one timestep. This ensures that nothing is left behind. The next grid point to advance is identified by using a binary tree algorithm for improved efficiency [6]. To enhance stability and efficiency, the hybrid method is used to advance the local currents [7]. The robust stability properties of the method lie in having the adjacent points values ahead of the central point in time when calculating the diffusion. The timestep size Δt_k^n is chosen at each timestep, using the first order expression for the local truncation errors of the membrane voltage and the fast sodium channel activation variable. Allowing larger local error leads to faster computing but lower precision.

The favorable stability properties of this algorithm allow the use of timesteps that are several orders of magnitude larger than the limit imposed in the FEFT. When using such large timesteps, the Courant Friedrich Levy (CFL) stability condition is often encountered, due to the explicit nature of the method. The CFL condition states that information cannot travel faster than the propagation velocity Vel for explicit methods. The condition therefore requires that $\Delta t < \Delta t_{CFL} = \Delta x/Vel$. However, timesteps larger than Δt_{CFL} can be used for regions where the diffusion is negligible (no communication between the cells), namely away from the upstroke and the repolarization phases. Cells ahead of the wavefront must, however, have a way to foresee the imminent approach of the wavefront so that they have time to reduce their timesteps accordingly. This can be achieved by limiting the spatial timestep variation to $1/Vel$. In other words, the timestep increment between any two adjacent points must be less than $\Delta t_{inc} < \Delta x/Vel$. Another problem is caused by the exponential nature of the dynamics in the AP upstroke. Any local error produced at the foot of the AP is drastically amplified, which results in large propagation velocity error. This can be avoided by using smaller timesteps at the foot of the AP than those calculated from the local truncation error considerations. This can be achieved using a nonlinear timestep increment $\Delta t_{inc}(x)$. For $dV/dt > 0.1/K_{guard}$, we use the expression:

$$\begin{aligned} \Delta t_{inc}(x) &= \frac{\overline{\Delta t}_{inc}}{1 + K_{guard}\left|dV/dt\right|} \\ &\leq \frac{\Delta x/Vel}{1 + K_{guard}\left|dV/dt\right|} \end{aligned} \qquad (4)$$

where K_{guard} is a constant. When $dV/dt < 0.1/K_{guard}$, we use $\Delta t_{inc}(x) = \overline{\Delta t}_{inc}$. By using such an expression, we impose a very small increment to the spatial timestep variation in front of the upstroke where dV/dt is large and positive. This creates a "protective zone" within which the timestep is kept small in order to accurately compute the foot of the AP. The constant K_{guard} are used to adjust the extent of the protective zone for optimum efficiency.

Given a certain spatial profile of the timestep, the guard cell algorithm (GCA) calculates a new timestep profile Δt_{guard} by limiting the timestep increment between two adjacent grid points by $\Delta t_{inc}(x)$. Δt_{guard} does not need to be updated at each timestep iteration. One can update and store the values Δt_{guard} at a given time interval Δt_{update}. Every new timestep computed will be then compared and reduced to Δt_{guard} if necessary. The update of Δt_{guard} can be performed at time intervals as large as ten times $\Delta x/Vel$ without significant impact on the accuracy. This reduces significantly the overhead associated with the GCA, which we find then, takes less than 5% of the total computational time.

3. Results

We tested the method on a two dimensional tissue using the LRd model. The grid spacing was chosen to be approximately equal to the cell size. This gives $\Delta x = 100$ μm for the longitudinal direction along the fibers and $\Delta y = 31.5$ μm in transverse direction. The diagonal coefficients of the diffusion tensor were chosen to be $D_x = 1/(C_x R_x)$ and $D_y = 1/(C_y R_y)$ with the physiological values $C_x = 0.13$ μF/cm for the membrane capacitance, $R_x = 79$ kΩ/cm for the axial resistance along the fibers and $R_y = 790$ kΩ/cm in the transverse direction. There are two cells in the y-direction and 1100 in the x-direction making the tissue 11.1cm in length. This length was chosen so as to contain a full AP. The AP size was about 10.2 cm. An AP was first generated at the left end of the tissue and was allowed to propagate freely to the right in the longitudinal direction. Then, a second stimulus was applied after 200 ms (APD is about 175 ms). The activity was recorded for 290 ms. A reference case considered as the exact solution against which our method were judged was obtained using the FEFT with a very small timestep. Using the above mentioned parameters, the FE diffusion stability

limit is equal to $\Delta t_{diff} = 0.027$ ms, and $\Delta t_{CFL} = 0.17$ ms. For optimum efficiency, the parameters for the GCA were chosen to be $K_{guard} = 1$ and $\overline{\Delta t}_{inc} = 0.025$ ms ($\Delta x/Vel = \Delta t_{CFL} = 0.17$ ms). Figure 1 shows a snapshot of typical AP propagation (panel A) and the corresponding timestep distribution (panel B). To focus on the regions of interest, only the AP in its depolarization phase and the trailing portion of the preceding wave are shown. The Figure shows the protective region around the upstroke as well as the cap imposed on the timestep variability (Δt_{guard} in solid line in comparison with Δt in dotted line). Note that timesteps much larger than Δt_{CFL} and Δt_{diff} are used.

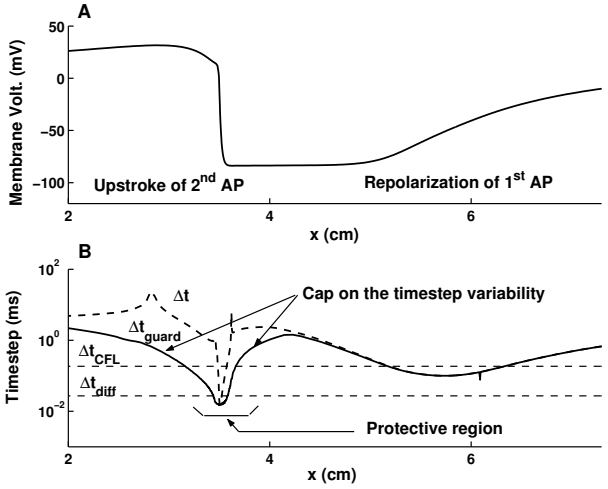

Figure 1. Snapshot of a propagating AP. Panel A shows the membrane voltage vs x. Panel B shows the corresponding spatial timestep distribution Δt (before applying the guard cell algorithm) and Δt_{guard} (after applying the guard cell algorithm). Note the use of small timesteps around the upstroke and the cap on the timestep variability. Note also the use of timesteps larger than Δt_{CFL} and Δt_{diff}

3.1. The guard cell methods

The increase in efficiency obtained by using the GCA is shown in Figure 2 panel A. The velocity errors were computed versus computational speed using the mBE (solid line) and compared to those obtained using the FEFT (dotted line). Since the computational efficiency is strongly dependent on the accuracy requirement, the results were computed by varying the local error tolerance. Speedup is normalized to the FEFT using a 5 μs timestep. To study the effect of the guard cell algorithm (GCA), results were obtained applying the mBE without the GCA (stars), with the linear version of the GCA using a constant value $\Delta t_{inc}(x) = \overline{\Delta t}_{inc}$ (squares) and with the nonlinear version of the GCA using $\Delta t_{inc}(x)$ (circles). Using the linear GCA, for a velocity error of 1%, the speed up is increased by about 50% compared to the case where no guard cells are used. This improvement results from the use of timesteps larger than Δt_{CFL}. When the nonlinear GCA is applied, resulting in a greater accuracy for computing the foot of the AP, we obtain an additional efficiency improvement of about 30% (line with circle markers compared with the line with square markers). Overall, given a certain velocity, the GCA improves the efficiency by 2 compared to the case where the GCA is not used.

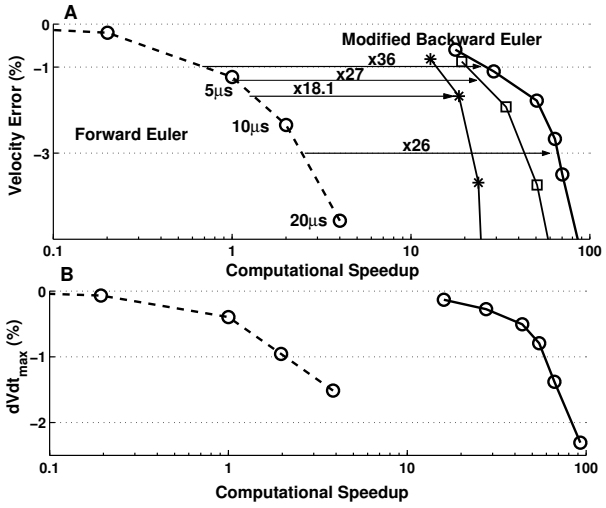

Figure 2. Efficiency comparison of mBE (solid line) vs. FEFT (dotted line). The velocity error (panel A) and $\dot{V}_{max}$ (panel B) are plotted versus computational speed. In panel A, results using the mBE are shown using the nonlinear GCA (circles), the linear GCA (squares) and without the GCA (stars). Number on top of arrows shows the efficiency improvement of mBE compared to FEFT at fixed velocity error.

3.2. Efficiency study

In order to further study the efficiency of the mBE, other characteristic properties of AP propagation including AP amplitude (APA), AP duration (APD), maximum membrane voltage (V_{max}) and $\dot{V}_{max}$ were also computed versus computational speed and compared to those obtained from the FEFT. Results are shown for $\dot{V}_{max}$ in Figure 2 panel B. $\dot{V}_{max}$ was typically the most error-sensitive property besides the velocity. The computational speed of the new algorithm was normalized to the speed of the FEFT method using a 5 μs timestep. Other characteristics are shown in Table 1 for two specific cases of -1% and -3% velocity error. We chose the velocity error as a comparison criterion, since it is usually the characteristic value that limits the overall efficiency of the algorithm. For a given

propagation velocity error, the mBE runs about 20–40 times faster than the FEFT. For $\dot{V}_{max}$, the accuracy is better or comparable to that obtained using FEFT for a given fixed propagation velocity error. The other characteristic values errors are below 1%, as shown in Table 1 for the cases of the velocity error equal to -1% and -3%. One can see that, overall, besides $\dot{V}_{max}$, the FE method is more accurate. This is not surprising since the FEFT used a very small fixed timestep, resulting in higher-than-required accuracy for APD, APA and V_{max} while providing only adequate accuracy for the velocity and $\dot{V}_{max}$. Even though mBE uses much larger timesteps away from the upstroke (cf. Figure 1), which results in a dramatic improvement in efficiency, mBE still manages to keep all errors aside from the velocity error within 1%, as shown in Table 1.

Table 1. CPU time and errors in AP characteristics for the mBE and FEFT, for a given velocity error equal to -1% and -3%.

	CPU time Speed Up	Vel.	APD	Errors V_{max}	(%) $\dot{V}_{max}$	APA
mBE	36	-1	-0.12	0.55	-0.52	-0.18
FEFT	1	-1	-0.01	0.00	-0.64	0.00
mBE	26	-3	-0.28	-0.89	-0.52	-0.30
FEFT	1	-3	0.00	-0.01	-2.04	0.00

The algorithm was also applied to the LRd model in two dimensions. We used the same cell size (100μ by $31.5\mu m$) and same tissue characteristics as in the one dimension simulation. The tissue was composed of 384 cells in longitudinal and 1100 cells in the transverse direction, totaling 422,400 cells. The tolerance was chosen so as to have the same unidirectional velocity propagation error as that obtained when using the FE with a timestep equal to 10 μs. The reentrant wave was induced using a cross-field stimulation. The efficiency using the mBE was improved by 20 in terms of CPU time in comparison with the FEFT. A snapshot of the spiral wave is shown in Figure 3 for both the FE in panel A and mBE in panel B. Overall the spiral wave characteristics agreed to within 1%. Panel C shows the timestep profile use to compute the mBE spiral shown in panel B. Note that most of the region uses timesteps larger than 0.3 ms.

4. Conclusion

The mBE method was shown to be highly stable allowing the use of timesteps much larger than the diffusion stability limit imposed by conventional explicit methods. The GCA allows the use of timesteps much larger than those defined by the CFL stability condition. It also creates a zone containing small timesteps at the foot of AP, which improves propagation velocity accuracy. Overall, for a given accuracy in velocity of 1% to 3%, the computational speed was increased by a factor of 30–40 over the FEFT, while the other errors were kept below 1%. The GCA alone, contributed a factor of two to this improvement.

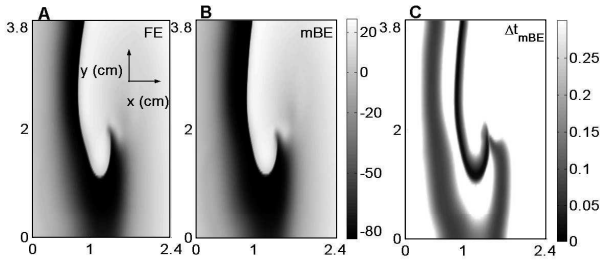

Figure 3. Simulation of a spiral using the FEFT (panel A) and mBE (panel B). No significant difference between the 2 methods can be seen. Panel C shows the timestep distribution related to the spiral computed with the mBE. For most of the tissue, large timestep beyond $0.3ms$ are used.

Acknowledgements

This work was supported by the Whitaker Development Award (3426162)

References

[1] Cherry EM, Greenside HS, Henriquez CS. A space-time adaptive method for simulating complex cardiac dynamics. Phys Rev Lett 2000;84:1343–1346.

[2] Quan W, Evans SJ, Hastings HM. Efficient integration of a realistic two-dimensional cardiac tissue model by domain decomposition. IEEE Trans Biomed Eng 1998;45:372–385.

[3] Qu Z, Garfinkel A. An advanced algorithm for solving partial differential equation in cardiac conduction. IEEE Trans Biomed Eng 1999;46:1166–1168.

[4] Lesh MD, Pring M, Spear JF. Cellular uncoupling can unmask dispersion of action potential duration in ventricular myocardium. Circ Res 1989;65:1426–1440.

[5] Luo CH, Rudy Y. A dynamical model of the cardiac ventricular action potential: I. simulations of ionic currents and concentration changes. Circ Res 1994;74:1071–1096.

[6] Otani NF. Computer modeling in cardiac electrophysiology. J of Comp Phys 2000;161:21–34.

[7] Rush S, Larsen H. A practical algorithm for solving dynamic membrane equations. IEEE Trans Biomed Eng 1966;13:389–392.

Address for correspondence:

Niels F. Otani
Dept. of Biomedical Engineering, CWRU
10900 Euclid Av, Cleveland OH 44106 / USA
nfo@po.cwru.edu